

## Seasonal variation for the ratio of BaP to BeP at different sites in Great Xiamen Bay

Shui-Ping Wu,<sup>\*a</sup> Ran-Ran Qian,<sup>a</sup> Tsung-Chang Lee,<sup>b</sup> Xing-Hong Wang,<sup>a</sup> Hua-Sheng Hong<sup>a</sup> and Chung-Shin Yuan<sup>ab</sup>

Received 18th October 2011, Accepted 20th February 2012

DOI: 10.1039/c2em10840b

From March 2008 to February 2009, PM<sub>10</sub> samples were collected and analyzed for polycyclic aromatic hydrocarbons (PAHs) at eight sampling sites in Great Xiamen Bay, China. Analyses of the seasonal and spatial variations of these compounds revealed the following results. Significantly high levels of PAHs were found in the winter compared to the summer, sometimes exceeding 100 ng m<sup>-3</sup>, and the spatial variations were influenced most by the sampling site surroundings. Composition profiles of PAHs of an urban and a rural site were shown to be very similar with a positive correlation coefficient larger than 0.9 at the 0.01 level of significance for the same season. Diagnostic ratios, together with principal component and multiple linear regression analysis, showed that more PAHs were from grass/wood/coal combustion in winter than in other seasons. The ratios of benzo[a]pyrene to benzo[e]pyrene (BaP–BeP) in winter and fall were 0.6–1.7 times higher than those in spring and summer, suggesting the importance of local emissions of PAHs. The BaP–BeP ratios in Kinmen were generally lower than those in Xiamen, indicating that the aging degree of PAHs was higher in Kinmen than in Xiamen. The external input of PAHs from upwind urban and industrial areas was one of the key factors causing high levels of PAHs in PM<sub>10</sub> in Great Xiamen Bay in winter.

### 1 Introduction

Much attention has been given to polycyclic aromatic hydrocarbons (PAHs) in urban airborne particulate matter in the past few decades, mainly due to the public health risks associated with the carcinogenic and mutagenic effects of PAHs.<sup>1–5</sup> Atmospheric PAHs are semi-volatile organic compounds (SVOCs), which are partitioned between the particulate and the gaseous phase. However, the carcinogenic high-molecular-weight ( $\geq 228$ ) PAHs are mostly associated with particulate matter.<sup>4,6,7</sup> Thus, it is

important to understand the occurrence and potential sources of PAHs associated with inhalable particulates (PM<sub>10</sub>) for health risk assessment. Because the concentrations of air pollutants are influenced by the emission sources,<sup>8–15</sup> atmospheric dynamics,<sup>16</sup> solar irradiation,<sup>9,10,14</sup> ambient temperature<sup>14,16</sup> and size distribution,<sup>13</sup> seasonal variations of particulate PAH concentrations, with highest values in winter,<sup>9–12,17–20</sup> are observed in many areas. However, it is difficult to differentiate the relative contribution of emission source variations and the thermal inversion effect to this seasonal variation.<sup>13,16,21</sup>

The Great Xiamen Bay, located at the southeastern coast of China and the west bank of Taiwan Strait, including Xiamen, Kinmen, part of Zhangzhou and Quanzhou, is an important engine of the Western Taiwan Straits Economic Zone. Nowadays, concurrent with the rapid growth in the economy and urbanization in the past years in Xiamen, as in many other areas

<sup>a</sup>State Key Laboratory of Marine Environmental Science, Xiamen University, Xiamen 361005, China. E-mail: [wsp@xmu.edu.cn](mailto:wsp@xmu.edu.cn); Fax: +86-592-2180655; Tel: +86-592-2188592

<sup>b</sup>Institute of Environmental Engineering, Sun Yat-Sen University, Kaosiung 80424, China

### Environmental impact

Understanding the influence of local emission and monsoons on the seasonal variation of PAHs associated with PM<sub>10</sub> in Great Xiamen Bay (mainly including Xiamen and Kinmen with completely different land use type, population and number of registered vehicles) is very important for regional air pollution management and control in the Western Taiwan Strait Economic Zone in China. Significantly higher levels of PAHs in PM<sub>10</sub>, as well as diagnostic ratios and HYSPLIT back trajectory, indicated that there was an external input of PAHs during the Northeastern Monsoon season. A very simple model was established to identify the influence of external input and thermal inversion on the high levels of PAHs in PM<sub>10</sub> during the Northeastern Monsoon season.

in China, the number of vehicles has increased significantly since 2003, from 275 000 vehicles to 620 000 vehicles in 2007, and the number is expected to reach 880 000 in 2012. Furthermore, pollution control policy steps are slow to follow the trends in emission increases. Air pollution has become one of the most worrying environmental problems in Xiamen, causing issues such as visibility impairment and acid rain.<sup>22–24</sup> Based on Xiamen Environmental Protection Bureau records, approximately 80% of days fell into the moderate/light pollution range based on API (air pollution index) levels and, in 2007, the responsible pollutant was PM<sub>10</sub>. Moreover, the monthly trends in the API levels in Xiamen coincided with the trend of PSI (pollution standards index, which is basically very close to the API used in Xiamen) in Kinmen very well from 2003 to 2007, with high levels from October to March (the northeast monsoon season).<sup>25</sup> Kinmen is mainly a tourist destination with a population density of around 5% of Xiamen's and has little industrial production. Besides the local emissions, the city of Jinjiang, with more than 700 ceramics factories (mainly coal-fired furnaces) in the northeast of Great Xiamen Bay, will influence the air in Great Xiamen Bay under the northeastern wind. The high levels of PM<sub>10</sub> (>100 µg m<sup>-3</sup>) found in Kinmen during the northeast monsoon seasons are likely to be the contributions from upwind pollution sources.<sup>26</sup> Similar seasonal variations of PM<sub>10</sub>, with low levels from June to August and high levels from October to March, in Great Xiamen Bay indicate that they are facing the same regional air pollution problems as those in the Great Beijing area, Yangtze River Delta (YRD), and Pearl River Delta (PRD) in China.<sup>25,27–29</sup>

The Great Xiamen Bay is under the influence of the East Asian monsoons and is characterized by a warm and wet summer monsoon and a cold and dry winter monsoon. In the winter, the winds are northeasterly and air pollutants from upwind industrial cities can be carried hundreds of kilometers or more by winds, resulting in air pollution episodes which fail air quality criteria.<sup>30</sup> However, the more often occurring thermal inversion can also result in the accumulation of air pollutants due to local emissions. Although the seasonal variations are reported in this area, the relative influence of external input of PAHs due to the influence of the northeast monsoon has not yet been identified.<sup>26,31,32</sup> As part of the Great Xiamen Bay Air Quality Monitoring Project, PM<sub>10</sub> samples were collected from eight sites in Great Xiamen Bay 2–5 times every month from March 2008 to February 2009 and analyzed for PAHs to improve our understanding of the combined influences of local emissions and monsoons on the seasonal variations of PAHs associated with PM<sub>10</sub>.

## 2 Experimental

### 2.1 Site selection and sampling

Eight sites located on building roofs in and around the Great Xiamen Bay were selected for the collection of PM<sub>10</sub> samples from March 2008 to February 2009 using PM<sub>10</sub> high-volume air samplers (KIMOTO 121FT, Japan and Laoying 2031, China) at an average flow rate of 1.0–1.2 m<sup>3</sup> min<sup>-1</sup> (Fig. 1). According to the local subtropical weather conditions, the year is divided into four seasons: spring (March, April and May), summer (June, July, August and September), fall (October and November) and winter (December, January and February). A total of 261 PM<sub>10</sub>

samples were collected. Sampling heights, samples per site and the surrounding environment are summarized in Table 1. Sampling sites, A2, A4 and A5, located in downtown Xiamen and Jinjing, are next to a street and likely to be influenced by the direct emissions from vehicle exhausts and cooking oil fumes. Site A1, located in the Zhangzhou campus of Xiamen University at the foot of green hills, has a more rural character. Air pollutants from Zhangzhou Harbour, Xiamen Harbour, Songyu power plant and the Xiamen urban area may influence air quality under northern wind conditions, whereas pollutants emitted from Houshi power plant may be transported to the site under southwesterly winds. A3, located at the small island of Dadeng in the Xiamen area, is a tourist area. Kinmen is recognized as a national park and the local air pollutants emissions are well controlled. Thus, three sites (B1, B2 and B3) in Kinmen are more likely to be influenced by regional air pollution, especially from the northern and northeastern industrial areas during the northeastern monsoon seasons.

PM<sub>10</sub> samples were collected on quartz filters (Pallflex 2500 QAT-UP, USA) with an approximate sampling time of 24 h. The quartz filters were baked in a Muffle furnace for 6 h at 600 °C and weighed (Sartorius 0.1 mg, Germany) after being conditioned in a desiccator. After sampling, the filters were separately wrapped in aluminum foil bags and weighed again after conditioning, and stored in a freezer at –20 °C until analysis. The meteorological factors including temperature, relative humidity (RH), wind direction, wind speed and rainfall (PH-1, XPH Co., China) during the sampling period were obtained from an air quality automatic monitoring station near the sampling site of B2 and A2 sampling sites.

### 2.2 Sample analysis

The method of extraction and cleanup was modified from US EPA method 3550B (ultrasonic extraction) and 3630C (silica gel cleanup).<sup>33</sup> One quarter of each filter paper was cut into 1 cm<sup>2</sup> squares and put into a centrifuge tube. 30 mL of dichloromethane (DCM, for trace organic analysis, Merck) was added and the mixture was sonicated three times for 45 min after soaking overnight. The combined supernatants were concentrated to approximately 10 mL under reduced pressure in a 20 °C water-bath using a rotary evaporator. An additional 15 mL hexane (Merck, 99% purity) was added to the flask for solvent exchange and the extract was concentrated again to approximately 1 mL. The concentrated extract was passed through a silica gel column with anhydrous sodium sulfate on the top. The column was successively eluted with 25 ml hexane followed by 40 ml hexane–DCM (6 : 4 v/v) to separate the alkanes and PAHs from the polar compounds. The PAH fraction was reduced to 200 µL using rotary evaporation and gentle high-purity N<sub>2</sub> was blow down. A known amount of hexamethylbenzene was added to the sample for PAH quantification as an internal standard before analysis using GC-MS.

19 PAHs (16 priority pollutants promulgated by the US EPA, plus benzo[e]pyrene, perylene and coronene) (AccuStandard Inc., USA) were analyzed using an Agilent 6890 GC coupled with an Agilent 5973 MSD operated in a selected ion monitoring mode. A 30 m × 0.25 mm i.d. × 0.25 µm HP5-MS capillary column (Agilent Co., USA) was used with an oven temperature

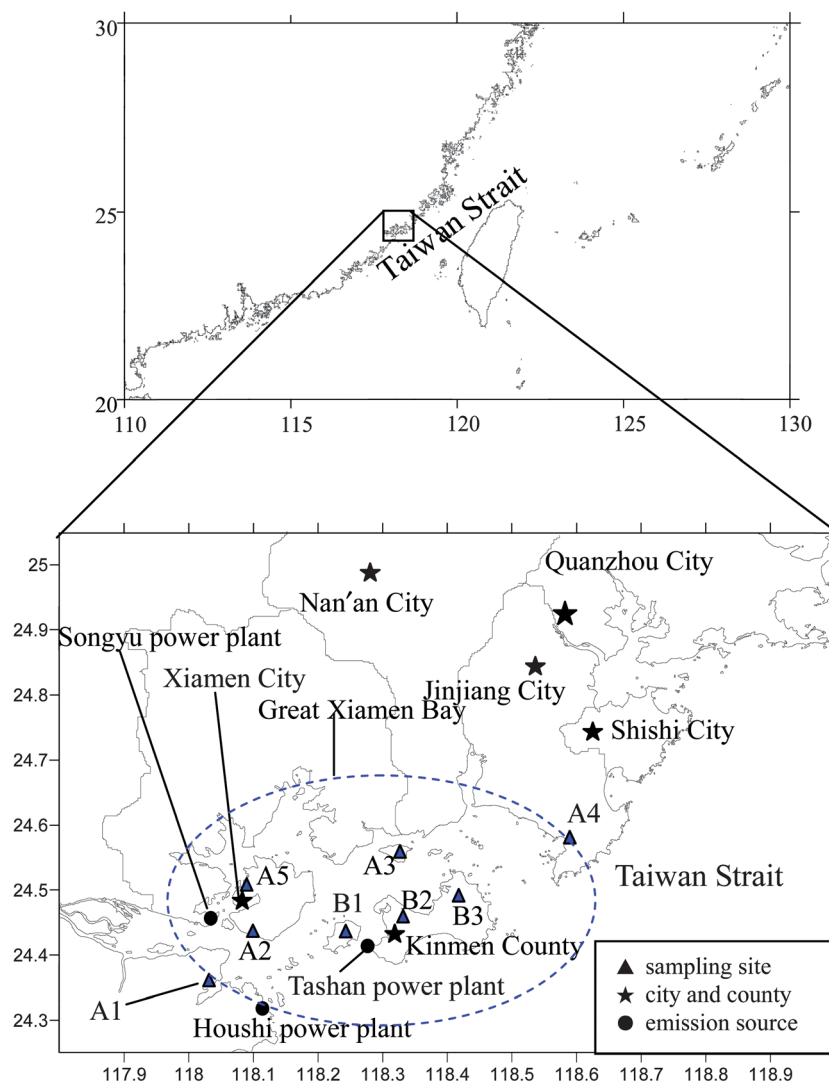


Fig. 1 Map of sampling sites and the three power plants.

program from 60 °C to 300 °C at a rate of 5 °C min<sup>-1</sup> (held isothermally at the end temperature for 20 min). Then, 1 µL of sample solution was injected in the splitless mode using an auto sampler. Ultrapure helium (99.999%) was used as the carrier gas for GC-MS. Five levels of mixed standard solutions of the 19 PAHs were used for the calculation of PAHs and the exact volume was corrected with hexamethylbenzene.

### 2.3 Quality control and quality assurance

Each sample was spiked with the deuterated PAH standard solution including naphthalene-d8 (Nap-d8), acenaphthene-d10 (Acp-d10), phenanthrene-d10 (Phe-d10), chrysene-d12 (Chr-d12) and perylene-d12 (Pery-d12) at a known volume before solvent extraction. Recoveries of the five PAH surrogate standards were as follows: 77 ± 6% for Nap-d8, 82 ± 7% for Acp-d10, 80 ± 8%

Table 1 Sampling locations and environmental descriptions for eight sampling sites

Sites	Sample locations	Latitude	Longitude	Altitude (m)	Descriptions	Number of samples
A1	Xiamen University Zhangzhou campus	24°22'48"	118°02'28"	45	Suburban area near mountain	35
A2	Xiamen University Ocean Building	24°26'08"	118°05'25"	21	Busy traffic and compact residential district	32
A3	Xiamen Dadeng middle school	24°33'33"	118°19'49"	14	Suburban area and close to farmland	30
A4	Jinjing Yuying primary school	24°34'34"	118°36'10"	18	Residential, factory and traffic mixture area	33
A5	Xiamen Huli central primary school	24°30'24"	118°05'56"	15	Residential/industrial/traffic mixture area	34
B1	Kinmen Lieyue middle school	24°25'50"	118°14'30"	34	Open area and naked field	31
B2	Kinmen Jinding primary school	24°26'53"	118°20'14"	30	Farmland and open area	33
B3	Kinmen Jinsha primary school	24°29'19"	118°24'43"	28	Open area and near a lake	33

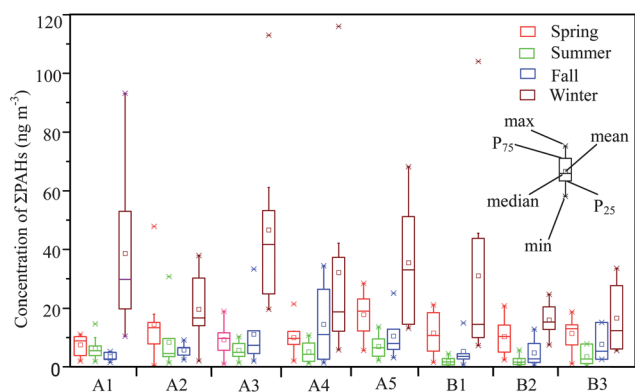


**Fig. 2** Seasonal variation of total PAHs in Great Xiamen Bay. The values of the maximum, the 75th, 50th (median), 25th percentile, and the minimum are illustrated by box-whisker symbols and the arithmetic means are presented as “□”.

for Phe-d10,  $92 \pm 12\%$  for Chr-d10, and  $82 \pm 8\%$  for Pery-d12. Field and laboratory blanks were also analyzed with the samples to check for any background contamination from artificial contaminants, reagents and glassware during the sampling and analytical procedure. There was not much difference in the PAH levels between the field and laboratory blanks, and both levels were less than 5% of the mass in the samples. The limits of detection (LODs) for each of the target compounds were calculated as the mean blank mass plus three standard deviations.<sup>34</sup> PAH compounds with molecular weight equal to or larger than 228 were not detected (ND) in the blanks. The LODs for the PAHs ranged from ND to  $126 \pm 17$  ng per sample for filter samples. The highest amounts found in the blanks were naphthalene ( $126 \pm 17$  ng per sample) and phenanthrene ( $22 \pm 3$  ng per sample). The much higher blank value for naphthalene was probably due to the emission of naphthalene from the toilet deodorant blocks next to the laboratory room. Sample quantities exceeding the LODs were quantified and corrected for blanks and recoveries. Water soluble inorganic ions and heavy metals in the same samples were also analyzed and are reported elsewhere.<sup>25</sup>

### 3 Results and discussion

#### 3.1 Temporal variations of PAHs

All 19 PAHs were determined in  $PM_{10}$  samples and the seasonal variations in total PAH concentrations ( $\Sigma$ PAHs) at eight sites in Great Xiamen Bay are shown in Fig. 2. The median value of  $\Sigma$ PAHs in winter were 0.3–10.2 times higher than those in other seasons (except the value of  $\Sigma$ PAHs at site B3 in spring) and the lowest levels were found in summer. As shown in Fig. 2, the levels of  $\Sigma$ PAHs could exceed  $100 \text{ ng m}^{-3}$  in winter. As discussed earlier, similar seasonal variations of PAHs were reported worldwide. More fossil fuel usage,<sup>14,18,19</sup> lower mixing height,<sup>14,18,19,30</sup> less solar radiation and photodegradation,<sup>18,30,35</sup> less rainfall and more gas-to-particle conversion<sup>14,16</sup> could result in these higher levels of PAHs in winter. However, higher temperature, higher mixing height, more frequent rainfall and more photodegradation are reported to be responsible for the lower levels of PAHs in other seasons, especially in

summer.<sup>12,14,17,21</sup> Although an external input of PAHs from upwind industrial and urban areas could also contribute to local air pollution, it is difficult to quantify its influence.<sup>13,16,21</sup> As mentioned earlier, Great Xiamen Bay has a subtropical East Asian monsoon climate and the seasonal variation of monsoons, solar radiation, and meteorological conditions could affect PAH levels in  $PM_{10}$ . Under southern and southwestern wind conditions in summer (Fig. 3), clean air mass from the ocean can dilute the local air pollutants and in turn leads to lower levels of PAHs, although the upwind power plants are potential emission sources (Fig. 1). Moreover, 57.9% of annual rainfall and 50.2% of annual total solar radiation occur during the summer season based on our observations. Thus, lower PAHs levels were likely to be attributed to the combination of favorable meteorological conditions, wash-out effects and losses due to photodegradation. On the contrary, in winter, the northeasterly wind brings in highly polluted air masses from the upwind urban and industrial area to the sampling sites. The mean temperature in winter ( $15.6 \text{ }^\circ\text{C}$ ) was much lower than that in summer ( $29.5 \text{ }^\circ\text{C}$ ) and only 2.5% of the annual rainfall and 14.5% of the annual total solar radiation occurs in winter. As the average wind speed in winter ( $3.7 \text{ m s}^{-1}$ ) was a little higher than that in summer ( $3.4 \text{ m s}^{-1}$ ), the wind speed could not be an important factor influencing the difference of the levels of PAHs in  $PM_{10}$  between summer and winter. The analysis on atmospheric mixing height of Xiamen showed that the average monthly mixing heights were highest in the months of October (1180 m), November (1120 m) and December (1040 m) and lowest in the months of April (810 m), May (780 m) and June (800 m).<sup>36</sup> Similar seasonal variations of mixing height, with higher values in winter and lower values in summer, were also reported in Guangzhou of Southern China.<sup>37</sup> In Great Xiamen Bay, there is little seasonal variation in emissions from stationary sources as domestic heating is unnecessary. Thus, the higher PAHs in winter were probably due to the input of external sources, less wash-out effects, gas-to-particle partitioning under cooler temperature and less photodegradation losses. The mixing height did not seem to be an important factor influencing the levels of PAHs in  $PM_{10}$  in Great Xiamen Bay.

It is reported that the spatial distribution of ambient PAHs were significantly correlated with the corresponding emission density or population density.<sup>38,39</sup> As can be seen in Fig. 2, the median values of  $\Sigma$ PAHs in  $PM_{10}$  were generally higher in Xiamen than those in Kinmen which correspond to the differences in population density between Kinmen and Xiamen. Although the A3 site is in a tourist area without strong vehicle emission, the highest median value of  $\Sigma$ PAHs was found ( $41.7 \text{ ng m}^{-3}$ ) in winter, suggesting that the external input of PAHs was very strong at this site. The intensive industrial areas with coal as the major energy source to the north of Dadeng Island were probably the major sources of PAHs in  $PM_{10}$  at site A3 in winter. However, much lower levels of  $\Sigma$ PAHs were observed at sites B1, B2 and B3 in Kinmen, probably due to the deposition and photodegradation losses as they were transported from the source to the sampling sites in winter. On the other hand, site A5 was a mixture of residential/industrial/traffic areas and the source strength of PAHs at this site was much higher than those at other sites. Although sites A2 and A4 are next to a street, the source strengths at the two sites were much lower than that at site A5 due to the lower volume of traffic. The emission from

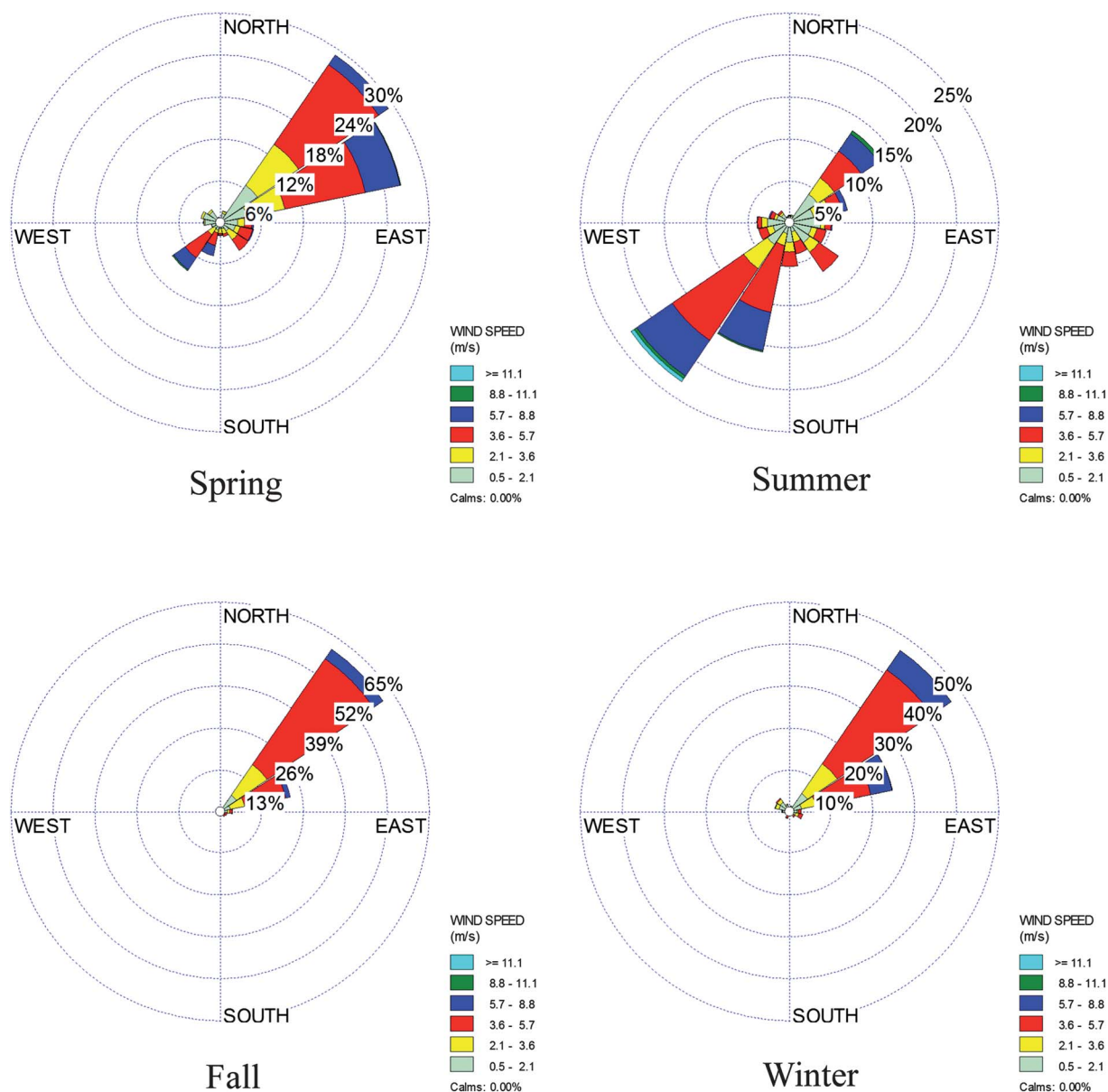


Fig. 3 Wind roses of different seasons in Great Xiamen Bay.

heavy-duty trucks used for sand and stone transfer in Zhangzhou harbor was probably an important source of PAHs at site A1 in winter. Based on the above analysis, the higher levels of PAHs in  $PM_{10}$  in winter were probably due to a combination of external input and meteorological conditions in Great Xiamen Bay. Thus, it is important to identify the source difference of PAHs for different seasons in order to quantify the relative influence of these two factors on the sharp increase of PAHs in winter.

### 3.2 Source identification of PAHs

Individual PAHs had very similar patterns at sites A5 and B2 in the same season, even though these two sampling sites had completely different local surroundings and human activities (Fig. 4 and Table 1), suggesting that these contaminants in Great Xiamen Bay were originally from a common local/

regional source. In contrast to spring and summer, 3- and 4-ring PAHs contributed 15.7–37.4% more to the  $\Sigma PAHs$  in fall and winter. Although low temperatures provided favorable conditions for the condensation/sorption of middle molecular weight PAHs to particles, the temperature in fall was on average 3.2 °C higher than that in spring and gas-to-particle partitioning shift due to temperature variation alone cannot explain the seasonal difference of profiles.<sup>40</sup> Therefore, the seasonal variations in emission sources needs to be identified. Various molecular diagnostic ratios of PAHs are widely used for their source identification.<sup>32,41–44</sup> It should be noted, however, that the ratios might change from emission sources to receptors due to the influences of photodegradation or aging,<sup>45,46</sup> and the direct application of these ratios requires the loss rates of the paired PAHs to be maintained close to each other during transportation in order to avoid incorrect source information.

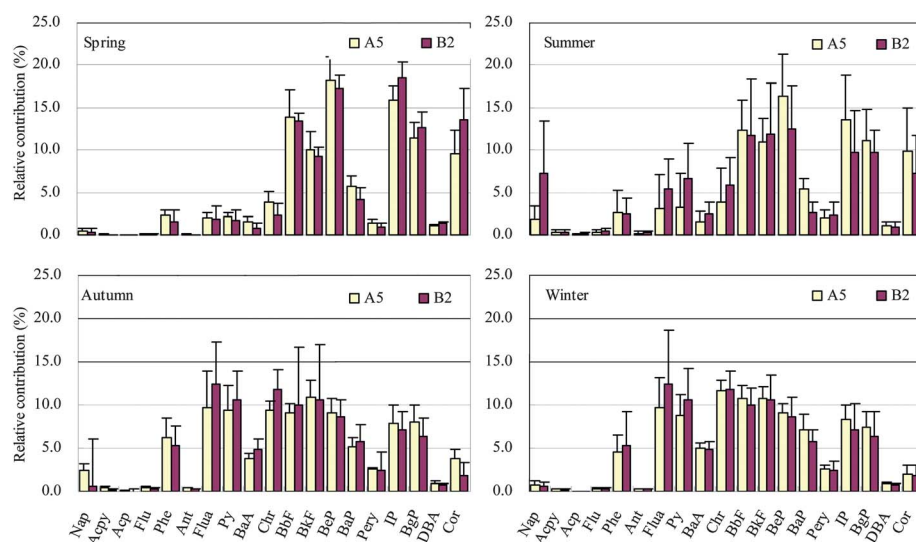


**Fig. 4** Comparison of PAH profiles between A5 and B2 for different seasons. naphthalene (Nap), acenaphthylene (AcPy), acenaphthene (Acp), fluorene (Flu), phenanthrene (Phe), anthracene (Ant), fluoranthene (Flua), pyrene (Py), benz[a]anthracene (BaA), chrysene (Chr), benzo[b]fluoranthene (BbF), benzo[k]fluoranthene (BkF), benzo[e]pyrene (BeP), benzo[a]pyrene (BaP), perylene (Pery), indeno[1,2,3-cd]pyrene (IP), dibenzo[a,h]anthracene (DBA), benzo[g,h,i]perylene (BgP) and coronene (Cor).

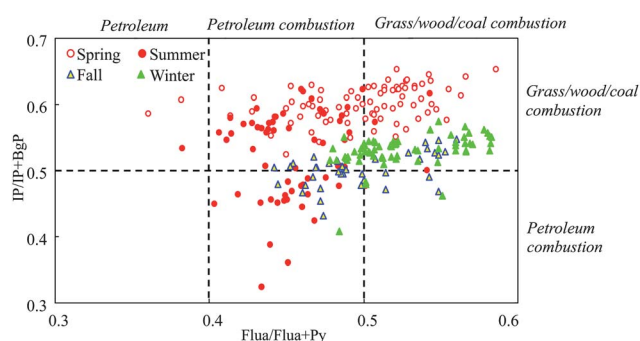


**Fig. 5** PAHs cross-plot for the ratio of Flua to Flua + Py vs. IP to IP + BgP in Great Xiamen Bay.

Source-diagnostic ratios of fluoranthene (Flua) to Flua plus pyrene (Py) ( $Flua/Flua + Py$ ) and indeno[1,2,3-cd]pyrene (IP) to IP plus benzo[g,h,i]perylene (BgP) ( $IP/IP + BgP$ ), due to their conservation during photodegradation, are used together to distinguish petroleum combustion from grass/wood/coal combustion.<sup>32,44,47</sup> In Great Xiamen Bay, the two ratios were calculated for different seasons and shown in Fig. 5. The spot distribution of 82% in winter samples in the cross plot was close to the area of grass/wood/coal combustion, while diagnostic ratios of other season samples suggested mixed emission sources of petroleum and grass/wood/coal combustion. This seasonal variation of diagnostic ratios revealed the seasonal variations of emission sources of PAHs with more emission from grass/wood/coal combustion in winter. In Great Xiamen Bay where there is no domestic heating in winter, the local emission sources of PAHs should vary little. Thus, the external input of PAHs, characterized with a grass/wood/coal combustion source from upwind industrial and urban areas under northeastern monsoon conditions, was a potential source of PAHs in Great Xiamen Bay in winter.

In order to quantify the relative contribution of different emission sources of PAHs, principal component analysis (PCA) plus multiple linear regression analysis (MLRA) are often carried out in the source identification of airborne PAHs.<sup>10,48</sup> The PCA method attempts to reduce the number of multivariate data whilst preserving most of the variance of the original data. In this study, data reduction was carried out using SPSS for Windows 10.0 with the orthogonal transformation method with varimax rotation and an eigenvalue whose magnitude is greater than unity, is retained. For the PAHs in Great Xiamen Bay, two principal components were identified in each season (Table 2). Factor 1 was mostly associated with high molecular weight PAHs including BbF, BkF, BeP, BaP, IP, BgP, DBA and Cor, and factor 2 was highly weighted in favor of middle molecular weight PAHs including Phe, Ant, Flua, Py, BaA and Chr. Emissions from gasoline exhausts are reported to be enriched in BeP, BaP, IP, BgP, DBA and Cor, while diesel exhausts are enriched in BbF and BkF, and Phe, Ant, Flua, Py, BaA and Chr, are tracers for coal combustion.<sup>49–51</sup> Therefore, factor 1, which accounted for 57.98–82.43% of the total variance, indicated that the main source of PAHs was vehicular emissions, including gasoline and diesel vehicular exhausts. Factor 2, accounting for 8.47–33.46% of the total variance, suggested that coal combustion was a major source of PAHs. In Great Xiamen Bay, factors 1 and 2 together explained >90% of the variance (Table 2), implying that the contribution of vehicular emissions was higher, or dominant, at the sampling sites. The PCA results were in good agreement with the source-diagnostic ratios.

The presence of Flua in air appears to be a marker for coal combustion, while the presence of BgP in air indicates vehicle emission as the source.<sup>48,52,53</sup> In light of our PCA results, BgP and Flua could be used as markers for vehicle exhausts and coal combustion sources, respectively. Then, taking the markers as independent variables ( $x$ ) and the sum concentration of PAHs as the dependent variable ( $y$ ), the mean contributions of principal

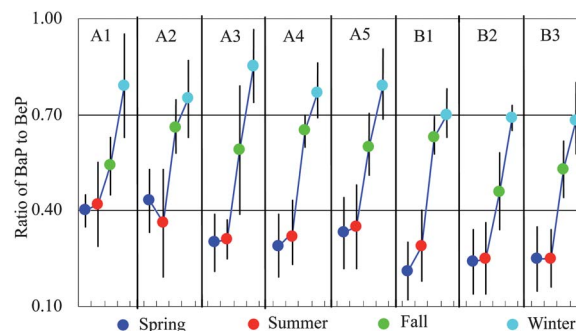
**Table 2** PCA analysis of PAHs in Great Xiamen Bay in different seasons<sup>a</sup>

	Spring		Summer		Fall		Winter	
	Factor 1	Factor 2	Factor 1	Factor 2	Factor 1	Factor 2	Factor 1	Factor 2
Phe		0.908		0.868		0.908		0.973
Ant		0.890		0.924	0.752			0.751
Flua		0.858		<b>0.984</b>		<b>0.943</b>		<b>0.982</b>
Py		0.884		0.977		0.890		0.970
BaA		0.897		0.955	0.681	0.686	0.810	
Chr		0.863		0.966		0.800	0.675	0.713
BbF	0.870		0.928		0.831		0.896	
BkF	0.837		0.857		0.850		0.910	
BeP	0.901		0.977		0.880		0.933	
BaP	0.609	0.759	0.887		0.817		0.921	
Pery		0.777		0.804	0.715		0.954	
IP	0.904		0.982		0.859		0.970	
BgP	<b>0.916</b>		<b>0.954</b>		<b>0.883</b>		<b>0.979</b>	
DBA	0.904		0.971		0.800		0.966	
Cor	0.879		0.957		0.934		0.889	
% Variance	77.83	13.28	57.98	33.46	82.43	8.47	74.35	19.27
Cumulative (%)	77.83	91.11	57.98	91.44	82.43	90.90	74.35	93.62
Source	Vehicle exhausts	Coal combustion	Vehicle exhausts	Coal combustion	Vehicle exhausts	Coal combustion	Vehicle exhausts	Coal combustion

<sup>a</sup> Extraction Method: Principal Component Analysis. Rotation Method: Varimax with Kaiser Normalization. Eigenvalue >1.0 and factor loading  $\geq 0.60$  are listed.

factors were calculated using MLRA (Table 3). A very good correlation was attained between observed and fitted values ( $R^2 > 0.9$ ,  $p < 0.001$ ). Table 3 shows that the emission sources of PAHs at PM<sub>10</sub> in Great Xiamen Bay had a seasonal variation, with a higher contribution from coal combustion in fall and winter in contrast to those in spring and summer. As discussed earlier, there was no seasonal variation in the local emission sources. The seasonal variation of PAHs sources was probably mainly related to monsoon variation and the external input of PAHs.

PAHs associated with particles are subjected to aging by chemical processes such as oxidation at the surface and bulk. The loss rate of PAHs depends on the molecular structure and particle substrate.<sup>45,46</sup> As discussed in the literature, BaP is expected to degrade more easily than its isomer BeP during transportation,<sup>54</sup> and the ratio of BaP to BeP (BaP–BeP) is widely used to ascertain the aging process, with higher values indicating freshly emitted PAHs.<sup>30,32,55–57</sup> A BaP–BeP ratio close to unity indicates negligible photochemical degradation and major impact from local emission sources, while lower ratios indicate more aged PAHs. In Great Xiamen Bay, the ratios were 0.6–1.7 times higher in winter and fall than those in spring and summer and the ratios were generally lower in Kinmen (B1–B3)

**Fig. 6** Seasonal variation for the ratio of BaP to BeP at different sites in Great Xiamen Bay.

than those in Xiamen (A1–A5) in the same season (Fig. 6), indicating that the aging degree of PAHs in Kinmen was generally higher than that in Xiamen. In other words, more PAHs in Kinmen were from external input in comparison with in Xiamen. The average values of  $\geq 0.7$  in winter indicated that the air masses were relatively fresh and not aged. It is reasonable to assume that the sources were mainly local and the impact of

**Table 3** Contribution of PAHs from vehicle exhausts and coal combustion<sup>a</sup>

Seasons	Regression equation	$R^2$	vehicle emission (%)	coal combustion (%)
Spring	$y = 6.047x_1 + 8.734x_2 + 0.92$	0.962	68.85	20.56
Summer	$y = 6.384x_1 + 7.722x_2 + 0.05$	0.918	85.20	13.57
Fall	$y = 8.186x_1 + 3.632x_2 + 0.018$	0.970	63.43	36.21
Winter	$y = 7.091x_1 + 3.705x_2 + 1.496$	0.975	52.42	42.86

<sup>a</sup>  $x_1$  and  $x_2$  represent the concentration of BgP and Flua, respectively.  $R^2$  is a measure of goodness-of-fit of linear regression.

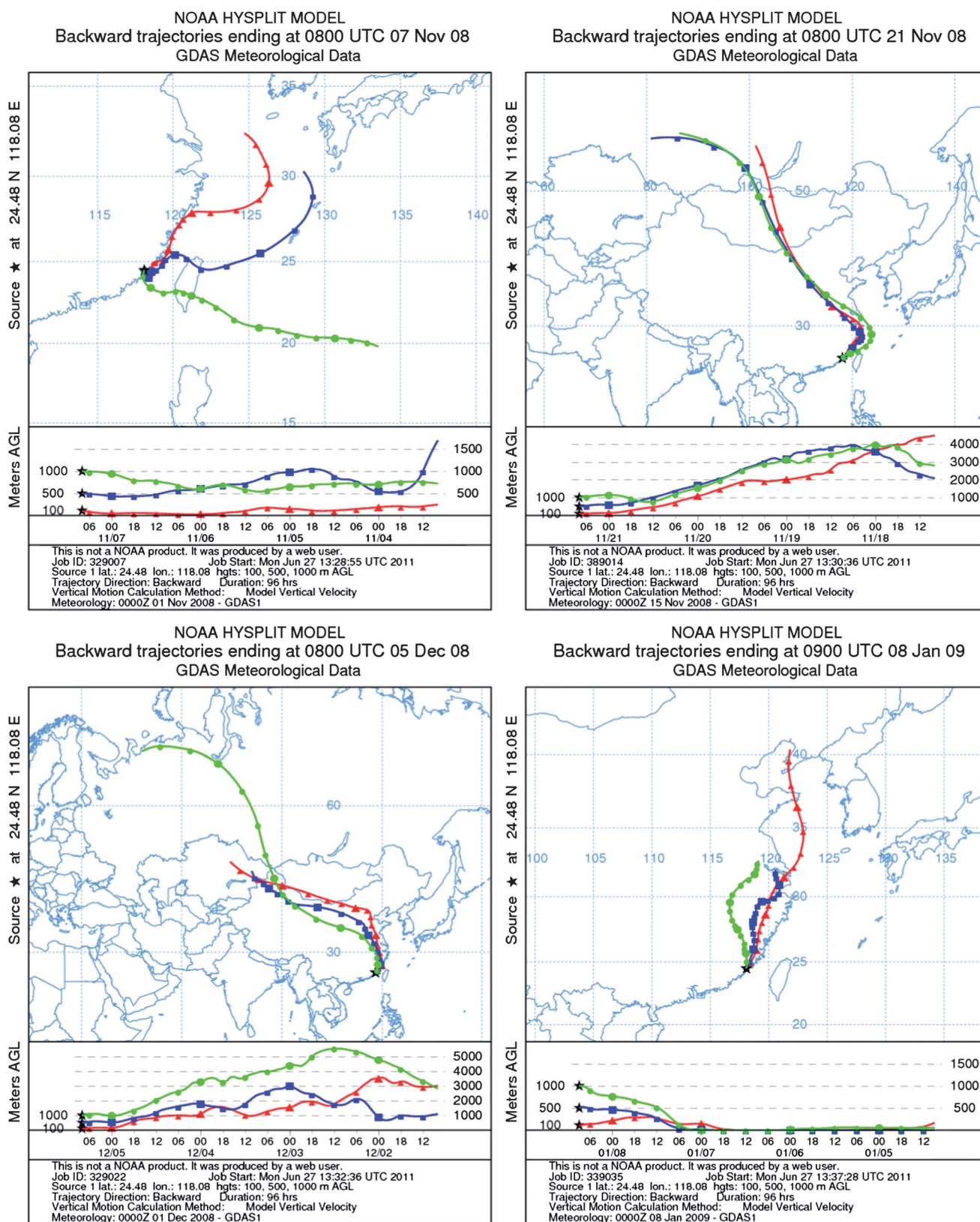


Fig. 7 Backward trajectories in northeastern monsoon season.

long-range transport was minor. The higher ratios of BaP–BeP were probably due to weak photo-degradation followed by the less solar radiation in fall and winter. The significantly positive

correlations ( $r = 0.541$  in winter and  $0.645$  in fall,  $p < 0.01$ ) found between  $\Sigma$ PAHs and BaP–BeP in fall and winter further emphasize that the major sources of PAHs in  $PM_{10}$  are from



local emissions in Great Xiamen Bay,<sup>32</sup> which is different from that observed in Hong Kong.<sup>10</sup>

### 3.3 Influence of the external input of PAHs

As discussed earlier, both local and regional emission sources could contribute to the PAHs in PM<sub>10</sub> in Great Xiamen Bay in winter. Southwesterly and southerly winds in summer bring in clean oceanic air masses which helps to dilute the pollutant levels, whereas the contaminated air mass from upwind urbanized and industrial areas under the northeastern monsoons in winter increased air pollution (Fig. 2 and Fig. 3). The Hybrid Single-Particle Lagrangian Integrated Trajectory is a widely used model that plots the trajectory of a single air parcel from a specific location and height above ground over a period of time. The 72-hour backward trajectories of air parcels that arrived at Great Xiamen Bay on four different days are shown in Fig. 7. When the air mass came from the East China Sea on 7 Nov. 2008, the average level of  $\sum$ PAHs reached 8.19 and 3.45 ng m<sup>-3</sup> in Xiamen and Kinmen, respectively. However, the average level of  $\sum$ PAHs increased to 18.45 and 14.38 ng m<sup>-3</sup> in Xiamen and Kinmen, respectively, when the air mass came from the mainland on 21<sup>st</sup> Nov. 2008. Generally, most cities in North China start their domestic heating (mainly coal-fired boilers) in the middle of November. It is possible that polluted air mass due to coal burning from North China contributed to the high levels of PAHs in Great Xiamen Bay under northeastern monsoons. In addition, the daily temperature on 21<sup>st</sup> Nov. 2008 (17 °C) was much lower than that on 7<sup>th</sup> Nov. 2008 (26 °C). The levels of PAHs would increase in case of thermal inversions formed at lower temperatures. Emissions from coal-burning stoves and furnaces (mainly in ceramic factories) in Nan'an and Jinjiang city to the north and northeast of Great Xiamen Bay would be transported to the downwind sites under northern and northeasterly winds. For example, the A3 site in Dadeng Island, with little industry and close proximity to the upwind ceramic industrial areas (Fig. 1), had the highest average concentration of  $\sum$ PAHs (42.8 ng m<sup>-3</sup>) in winter (Fig. 2). The 72-hour backward trajectories on 4<sup>th</sup> Dec. 2008 and 7<sup>th</sup> Jan. 2009 illustrated in Fig. 7 also show the mainland sources of the air mass.

Because of both additional external inputs and the decrease of temperature contributed to PAH concentrations, it is important to find a way to identify the contribution of these two main factors to this increase. However, the estimation of external input for PAHs in PM<sub>10</sub> in the Great Xiamen Bay is impossible due to the absence of the regional emission inventory of PAHs and the meteorological field. In the future, the regional emission inventory of PAHs is required to be estimated based on the reported emission activity and emission factor data,<sup>58</sup> and then the Community Multiscale Air Quality modeling system can be used to simulate the external input of PAHs in different seasons,<sup>59</sup> especially during severe winter air pollution episodes.<sup>26,60</sup>

## 4 Conclusions

Based on our results, we drew the following conclusions:

(1) PAHs associated with PM<sub>10</sub> at eight sites in Great Xiamen Bay showed significant seasonal variations with much higher

levels in winter, and the levels of these compounds in Kinmen were generally lower than those in Xiamen in the same season.

(2) Source-diagnostic ratios together with PCA and MLRA results showed that there was seasonal variation of PAHs emission sources in Great Xiamen Bay. Because there is little seasonal variation in the local emission from stationary sources, external input of PAHs from upwind urban and industrial areas was an important factor that led to increased levels of PAHs in PM<sub>10</sub> in Great Xiamen Bay during the northeast monsoon season.

(3) The effect of atmospheric mixing height on the levels of PAHs in PM<sub>10</sub> need to be identified in order to estimate the influence of lower temperature on the accumulation of PAHs in PM<sub>10</sub> in the future. Further studies are needed to investigate the regional-scale influences of the rapid development of urban agglomerations on air quality in China.

## Acknowledgements

This study was supported in part by the National Natural Science Foundation of China (40971257, 41171365), the Environmental Nonprofit Research and Special Project of China (201009004) and the Program for Changjiang Scholars and Innovative Research Team in University (PCSIRT). Professor John Hodgkiss of The University of Hong Kong is thanked for his help with English.

## References

- 1 B. Finlayson-Pitts and J. N. Pitts, *Science*, 1997, **276**, 1045–4051.
- 2 M. Zheng, M. Fang, F. Wang and K. L. To, *Atmos. Environ.*, 2000, **34**, 2691–2702.
- 3 S. C. Lee, K. F. Ho, L. Y. Chan, B. Zielinska and J. C. Chow, *Atmos. Environ.*, 2001, **35**, 5949–5960.
- 4 X. Bi, G. Sheng, P. Peng, Y. Chen, Z. Zhang and J. Fu, *Atmos. Environ.*, 2003, **37**, 289–299.
- 5 Y. Kameda, J. Shirai, T. Komai, J. Nakanishi and S. Masunaga, *Sci. Total Environ.*, 2005, **340**, 71–80.
- 6 A. Cincinelli, M. D. Bubba, T. Martellini, A. Gambaro and L. Lepri, *Chemosphere*, 2007, **68**, 472–478.
- 7 P. Spezzano, P. Picini and D. Cataldi, *Atmos. Environ.*, 2009, **43**, 539–545.
- 8 A. M. Caricchia, S. Chiavarini and M. Pezza, *Atmos. Environ.*, 1999, **33**, 3731–3738.
- 9 E. Menichini, F. Monfredini and F. Merli, *Atmos. Environ.*, 1999, **33**, 3739–3750.
- 10 H. Guo, S. C. Lee, K. F. Ho, X. M. Wang and S. C. Zou, *Atmos. Environ.*, 2003, **37**, 5307–5317.
- 11 Z. G. Guo, L. F. Sheng, J. L. Feng and M. Fang, *Atmos. Environ.*, 2003, **37**, 1825–1834.
- 12 J. Y. Lee, Y. P. Kim, N. Kaneyasu, H. Kumata and C.-H. Kang, *Atmos. Res.*, 2008, **90**, 91–98.
- 13 J. Duan, X. Bi, J. Tan, G. Sheng and J. Fu, *Chemosphere*, 2007, **67**, 614–622.
- 14 Y. W. F. Tham, K. Takeda and H. Sakugawa, *Atmos. Res.*, 2008, **88**, 224–233.
- 15 Y. Zhang and S. Tao, *Environ. Pollut.*, 2008, **156**, 657–663.
- 16 K. Ravindra, E. Wauters, van and R. Grieben, *Sci. Total Environ.*, 2008, **396**, 100–110.
- 17 M. Xie, G. Wang, S. Hu, Q. Han, Y. Xu and Z. Gao, *Atmos. Res.*, 2009, **93**, 840–848.
- 18 W.-L. Ma, Y.-F. Li, H. Qi, D.-Z. Sun, L.-Y. Liu and D.-G. Wang, *Chemosphere*, 2010, **79**, 441–447.
- 19 F. Tian, J. Chen, X. Qiao, Z. Wang, P. Yang, D. Wang and L. Ge, *Atmos. Environ.*, 2009, **43**, 2747–2753.
- 20 M. Amodio, M. Caselli, G. Gennaro and M. Tutino, *Environ. Res.*, 2009, **109**, 812–820.
- 21 D. W. M. Sin, Y. C. Wong, Y. Y. Choi, C. H. Lama and P. K. K. Louie, *J. Environ. Monit.*, 2003, **5**, 989–996.

- 22 J. X. Liu, C. C. Lin, Y. Y. Cai, Z. Lin and Z. L. Wang, *J. Trop. Meteor.*, 2007, **23**, 53–58.
- 23 L.-X. Zheng, S.-L. Zhang, L.-L. Chen and S.-J. Shi, *J. Anhui Agri. Sci.*, 2008, **36**, 13764–13765 (in Chinese with English abstract).
- 24 X.-Q. Fan and Z.-B. Sun, *Transactions Atmos. Sci.*, 2009, **32**, 604–609 (in Chinese with English abstract).
- 25 T.-C. Lee, *Physicochemical characteristics and source apportionment of atmospheric particles in Kinmen-Xiamen region*. Master thesis, Kaohsiung: National Sun Yat-Sen University, 2009.
- 26 S. C. Hsu, S. C. Liu, F. Tsai, G. Engling, I. I. Lin, K. C. Chou, S. J. Kao, S. C. C. Lung, C. Y. Chan, S. C. Lin, J. C. Huang, K. H. Chi, W. N. Chen, F. J. Lin, C. H. Huang, C. L. Kuo, T. C. Wu and Y. T. Huang, *J. Geophys. Res.*, 2010, **115**, D17309.
- 27 M. Shao, X. Tang, Y. Zhang and W. Li, *Front. Ecol. Environ.*, 2006, **4**, 353–361.
- 28 L. Li, C. H. Chen, C. Huang, H. Y. Huang, Z. P. Li, J. S. Fu, C. J. Jang and D. G. Streets, *Huan Jing Ke Xue*, 2008, **29**, 237–245 (in Chinese with English abstract).
- 29 Y. H. Zhang, M. Hu, L. J. Zhong, A. Wiedensohler, S. C. Liu, M. O. Andreae, W. Wang and S. J. Fan, *Atmos. Environ.*, 2008, **42**, 6157–617.
- 30 J. Li, G. Zhang, X. D. Li, S. H. Qi, G. Q. Liu and X. Z. Peng, *Sci. Total Environ.*, 2006, **355**, 145–155.
- 31 H. Hong, H. Yin, X. Wang and C. Ye, *Atmos. Res.*, 2007, **85**, 429–441.
- 32 S.-P. Wu, X.-H. Wang, J.-M. Yan, M.-M. Zhang and H. S. Hong, *Aerosol Air Qual. Res.*, 2010, **10**, 497–506.
- 33 US EPA, *Test Method for Evaluating Solid Waste - Physical/Chemical Methods*, SW-846, 1995, Washington, DC, USA.
- 34 S. P. Wu, S. Tao, F. L. Xu, R. Dawson, T. Lan, B. G. Li and J. Cao, *Sci. Total Environ.*, 2005, **345**, 115–126.
- 35 G. Wang, J. Li, C. Cheng, S. Hu, M. Xie, S. Gao, B. Zhou, W. Dai, J. Cao and Z. An, *Atmos. Chem. Phys.*, 2011, **11**, 4221–4235.
- 36 X. F. Wang, *Xiamen Sci Technol.*, 2010, **89**, 57–60 (in Chinese).
- 37 S. J. Fan, W. Zhu, A. Y. Wang, L. L. Guo and J. Dong, *Acta Sci. Natur. Univ. Sunyatseni*, 2005, **44**, 99–102.
- 38 S. Z. Liu, S. Tao, W. X. Liu, H. Dou, Y. N. Liu, J. Y. Zhao, M. G. Little, Z. F. Tian, J. F. Wang, L. G. Wang and Y. Gao, *Environ. Pollut.*, 2008, **156**, 651–656.
- 39 W. D. Hafner, D. L. Carlson and R. A. Hites, *Environ. Sci. Technol.*, 2005, **39**, 7374–7379.
- 40 Z. Gu, J. Feng, W. Han, L. Li, M. Wu, J. Fu and G. Sheng, *J. Environ. Sci.*, 2010, **22**, 389–396.
- 41 C. Venkataraman, J. M. Lyons and S. K. Friedlander, *Environ. Sci. Technol.*, 1994, **28**, 555–562.
- 42 W. E. Cotham and T. F. Bidleman, *Environ. Sci. Technol.*, 1995, **29**, 2782–2789.
- 43 C. Alves, C. Pio and A. Duarte, *Atmos. Environ.*, 2001, **35**, 5485–5496.
- 44 M. B. Yunker, R. W. Macdonald, R. Vingarzan, R. H. Mitchell, D. Goyette and S. Sylvestre, *Org. Geochem.*, 2002, **33**, 489–515.
- 45 X. L. Zhang, S. Tao, W. X. Liu, Y. Yang, Q. Zuo and S. Z. Liu, *Environ. Sci. Technol.*, 2005, **39**, 9109–9114.
- 46 D. Kim, B. M. Kumfer, C. Anastasio, I. M. Kennedy and T. M. Young, *Chemosphere*, 2009, **76**, 1075–1081.
- 47 W. F. Rogge, L. M. Hildemann, M. A. Mazurek, G. R. Cass and B. R. T. Simoneit, *Environ. Sci. Technol.*, 1993, **27**, 2700–2711.
- 48 R. M. Harrison, D. J. T. Smith and L. Luhana, *Environ. Sci. Technol.*, 1996, **30**, 825–832.
- 49 A. H. Miguel, T. W. Kirchstetter, R. A. Harley and S. Hering, *Environ. Sci. Technol.*, 1998, **32**, 450–455.
- 50 N. R. Khalili, P. A. Scheff and T. M. Holsen, *Atmos. Environ.*, 1995, **29**, 533–542.
- 51 P. Kulkarni and C. Venkataraman, *Atmos. Environ.*, 2000, **34**, 2785–2790.
- 52 S.-P. Wu, S. Tao, Z.-H. Zhang, T. Lan and Q. Zuo, *Environ. Pollut.*, 2007, **147**, 203–210.
- 53 X. Liu, G. Zhang, J. Li, H.-R. Cheng, S.-H. Qi, X.-D. Li and K. C. Jones, *J. Environ. Monit.*, 2007, **9**, 1092–1098.
- 54 T. Nielsen, *Atmos. Environ.*, 1988, **22**, 2249–2254.
- 55 X. Ding, X. M. Wang, Z. Q. Xie, C. H. Xiang, B. X. Mai, L. G. Sun, M. Zheng, G. Y. Sheng, J. M. Fu and U. Pöschl, *Atmos. Environ.*, 2007, **41**, 2061–2072.
- 56 F. Esen, Y. Tasdemir and N. Vardar, *Atmos. Res.*, 2008, **88**, 243–255.
- 57 M. S. Callén, M. T. de la Cruz, J. M. López, R. Murillo, M. V. Navarro and A. M. Mastral, *Water, Air, Soil Pollut.*, 2008, **190**, 271–285.
- 58 Y. X. Zhang and S. Tao, *Atmos. Environ.*, 2009, **43**, 812–819.
- 59 S. Wang, M. Zhao, J. Xing, Y. Wu, Y. Zhou, Y. Lei, K. He, L. Fu and J. Hao, *Environ. Sci. Technol.*, 2010, **44**, 2490–2496.
- 60 X. An, T. Zhu, Z. Wang, C. Li and Y. Wang, *Atmos. Chem. Phys. Discuss.*, 2006, **6**, 8215–8240.